Atmospheric remote sensing using multi-channel ground-based microwave radiometer

LEI Lianfa, LU Jianping, ZHU Lei, WU Hao

Xi'an Electronic Engineering Research Institute, Xi'an 710100, *China*

Abstract: This paper proposes a self-developed multi-channel ground-based microwave radiometer that uses a brightness temperature and data inversion method. We compared the radiometer data and the radiosonde observations, and then analyzed the radiometer observations in terms of brightness temperature, inversion temperature, and water vapor profile accuracy. Results show that the microwave radiometer has a small observation error of brightness temperature and the neural network inversion profiles of atmospheric temperature, water vapor, and other parameters are accurate and reliable. The proposed radiometer has practical applications.

Key words: microwave radiometer, BP neural network, MonoRTM model, multi-channel, groud-based

CLC number: P407.7 **Document code:** A

Citation format: Lei L F, Lu J P, Zhu L and Wu H. 2014. Atmospheric remote sensing using multi-channel ground-based microwave radiometer. Journal of R emote Sensing, 1 8(1): 180 – 191 [DOI: 10.11834/jrs.20133013]

1 INTRODUCTION

Atmospheric temperature, water vapor, relative humidity, and cloud liquid water profiles are the basic parameters used to describe the conditions of atmosphere; thus, detecting the spatial and temporal changes in these atmospheric parameters is essential in numerical weather prediction, climate change study, and various meteorological applications (Liu, et al., 2010). A sounding balloon is a main tool for detection but it is limited by many factors such as sparse spatial and temporal coverage. A ground-based microwave radiometer is an important, recently d eveloped atmospheric sounding equipment for observing tropospheric temperature, water vapor, clouds, and other atmospheric parameters, and it can overcome a number of limitations involve in atmospheric sounding applications, as well as obtain novel valuable meteorological data for the study of the atmospheric structure (Zhang, 2011; Meijgaard, et al., 2007). A microwave radiometer is commonly used in small-scale weather observations to continuously and automatically obtain troposphere atmospheric temperature, relative humidity, water vapor, liquid water, and other atmospheric parameters. These functions of the microwave radiometer make it important for weather forecasts, weather modification, flood control command decisions, atmospheric environmental research, and so on (Zhao, et al., 2009). In addition, the ability of the microwave radiometer to work independently in all-time, all-weather conditions, as well as to penetrate the clouds, makes it suitable in an automatic weather station. The capability of microwave radiometers to obtain continuous temperature, relative humidity, water vapor, liquid water, and other profile information is considered to be valuable for r etrieving a continuous vertical structure of the atmosphere, which can be used to improve the capacity of both short-term prediction and air pollution monitoring (Liu, et al., 2007).

Ground-based microwave radiometer data inversion mainly utilizes observed brightness temperatures to invert atmospheric temperature, water vapor, relative humidity, cloud liquid water, and other atmospheric parameters. Inversion methods include positive model inversion method, statistical method (empirical method), and artificial neural network method. In the comparison of the temperature, water vapor, and cloud liquid water profiles from the microwave radiometer data acquired using these a pproaches, results show that the artificial neural network method has superior functions which many traditional algorithms do not have. The three-layer neural network can theoretically fit any complex nonlinear modeling with sufficient accuracy. Analyzing the complex physical model using neural networks is thus unnecessary (Liu, et al., 2010; Shi, et al., 2009). We can directly use historical data to train the network. This artificial neural n etwork method is increasingly used in atmospheric science and other fields because of its ability to self-learn and to deal with nonlinear problems.

2 MICROWAVE RADIOMETER PROFILE

A microwave radiometer is a passive microwave remote sensing device. Although it does not emit electromagnetic waves, it can passively receive radiation from the targets to detect characteristics.

The atmosphere selectively absorbs the microwaves that pass through it. Fig. 1 shows the absorption spectra of cloud, water vapor, and oxygen. As shown in Fig. 1, the vapor resonance is

Received: 2013-01-23; **Accepted:** 2013-07-09; **Version of record first published:** 2013-07-16

Foundation: China Special Fund for Meteorological Research in the Public Interest (No. GYHY201006030)

First author biography: LEI Lianfa (1985—), male, master candidate, he majors in atmospheric remote sensing. E-mail: leilianfa_2006@163.com

at 22 GHz, and the atmospheric oxygen resonance is at 60 GHz. Thus, the vertical distribution of water vapor and o xygen can be obtained by measuring the radiation intensity or brightness temperature of water vapor and oxygen in the atmosphere near the 22 GHz and 60 GHz resonances (Marzano, et al., 2005; Yao, et al., 2005). The microwave radiometer inversion method can invert precision atmospheric profile parameters using artificial neural network combined with a considerable amount of historical radiometer data (Cerewell, et al., 2011; Domenico, e t al., 2007).

In this paper, data obtained from a newly self-developed multi-channel microwave radiometer for atmospheric remote sensing were used to invert parameters. A microwave radiometer is an accurate atmospheric detection device used for continuous monitoring of ambient air over the surface. Based on a previous study on troposphere radiative properties, 35 atmospheric sounding frequency points, 21 probe frequency points in the K-band (22—30 GHz), and 14 probe frequency points in the V-band (51—59 GHz) were set up. The proposed instrument accurately measured and obtained atmospheric radiation brightness temperature values using completely passive detection methods and these frequency scanning receivers. Finally, we detected the water vapor and liquid water contents of the atmosphere, as well as obtained continuous, high-resolution profiles of atmospheric temperature, water vapor, and other atmospheric parameters by means of real-time inversion using the artificial neural network algorithm combined with a large number of radio history radiosonde data. Microwave radiometer provides important observational data and decision support for numerical weather prediction, weather modification operations, and so on.

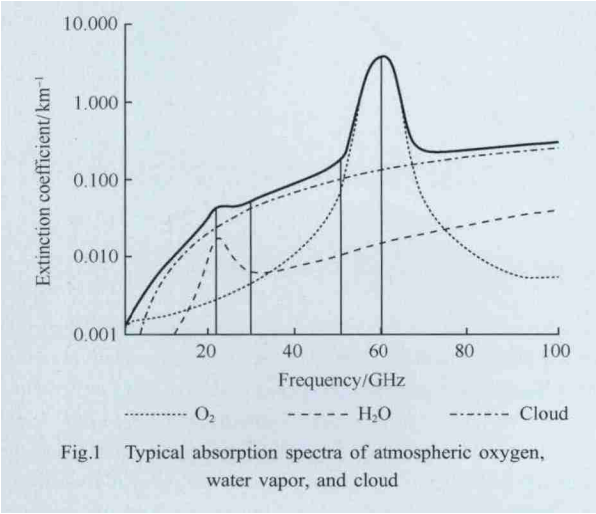

Fig.1 Typical absorption spectra of atmospheric oxygen, water vapor, and cloud

3 NEURAL NETWORK DESIGN AND ANALYSIS

The widely used and more mature three layer error Back Propagation (BP) neural network model algorithm was used in our experiment. In the neural network training process, ground-based observations of meteorological parameters (including ground temperature, barometric pressure, and relative humidity) and the frequency radiometer observations of brightness temperature were used as input. Temperature, relative humidity, and cloud liquid water profiles corresponding to 58 nodes in different networks were considered as output. A considerable number of local radiosonde data were taken as the training samples for n etwork training. A set of best matching network parameters was then obtained. The trained network can be directly used for microwave radiometer atmospheric temperature, water vapor, liquid water, and other profile retrievals in the following process. The experimental observation site is China National Meteorological Bureau in Beijing. We conducted two-month continuous observation experiments from September, 2012 to early November, 2012. Historical radiosonde data from a sounding station located in Beijing's suburbs were used for the neural network training. Precision instrument observation data retrieval and accuracy a nalysis were conducted as well.

4 EXPERIMENTAL RESULTS

4.1 Analysis and comparison of brightness temperatures

Given that brightness temperature cannot be measured d irectly from the radiosonde, brightness temperature simulation should be performed using an atmospheric radiation model. The atmospheric radiation model MonoRTM for brightness temperature simulation (Liu, el al., 2010; Clough, et al., 2004) was used in our simulation. Soundings can only have two observations every day, that is, once in the morning and once in the evening; thus, the amount of data that can be obtained was limited. Moreover, it took approximately 30 minutes for the balloons to rise up to 10 km. Therefore, we selected the average of the output brightness temperature from the radiometer in sounding hours and the brightness temperature computed by radiosonde data simulation for the comparative analysis.

The *BIAS* and Root Mean Square (*RMS*) of observed value and the true value (sounding simulation) are defined as

$$BIAS = \frac{1}{n}\sum_{i=1}^{n}(X_{i,\mathrm{meas}} - X_{i,\mathrm{true}}) \quad (1)$$

$$RMS = \sqrt{\frac{1}{n}\sum_{i=1}^{n}(X_{i,\mathrm{meas}} - X_{i,\mathrm{true}})^2} \quad (2)$$

where n indicates the number of observing samples, and $X_{i,\mathrm{meas}}$ and $X_{i,\mathrm{true}}$ represent the observed value and the true value, r espectively. A total of 69 groups of detection data samples from the radiometer and soundings of the same instant were selected in this test for the analysis and comparison of the results from September 10, 2012 to October 20, 2012. Fig. 2(a) (b) represent the *BIAS* and *RMS* of observed brightness temperature and simulated brightness temperature in the K and V bands, respectively.

Fig. 2(a) shows the *BIAS* in the K spectrum band. Although the *BIAS* was 1.6 K in the water vapor absorption peak, whereas it was only 1 K elsewhere, mainly because the effect of water v apor was stronger at this peak. An empirical model should be used to estimate perceptible water and cloud liquid water contents when MonoRTM model is used to compute for brightness temperature (Chen, 1989). However, the limitation of these estimation methods includes estimation results that are slightly less accurate. This limitation affects the simulation precision of the brightness temperature, leading to a larger average frequency deviation. Even though the measurement error of the

V band was larger than that of the K band, the average relative deviation of brightness temperature was less than 2.5%, which was relatively less.

Fig. 3(a)(b) show the linear correlation between observation atmospheric radiation brightness temperature and computation simulating brightness temperature in K and V spectrum bands, respectively. The result shows a high consistency between these parameters. The accuracy of brightness temperature measurements using the microwave radiometer was credible. This accuracy directly affected the precision of the follow-up neural network inversion algorithm. Therefore, the antinoise ability and observation accuracy of the instrument should be further improved.

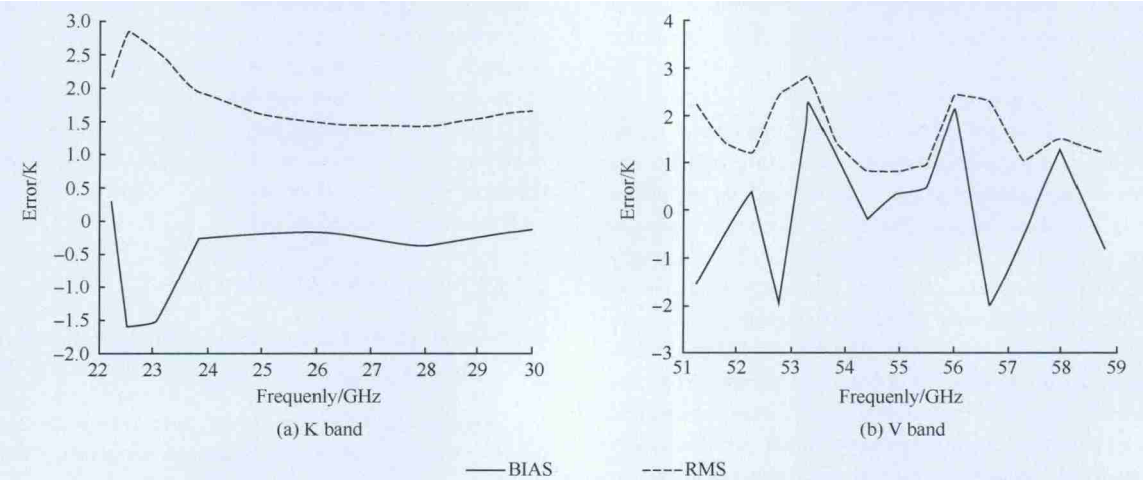

Fig.2 BIAS and RMS of observation brightness temperature and simulated brightness temperature

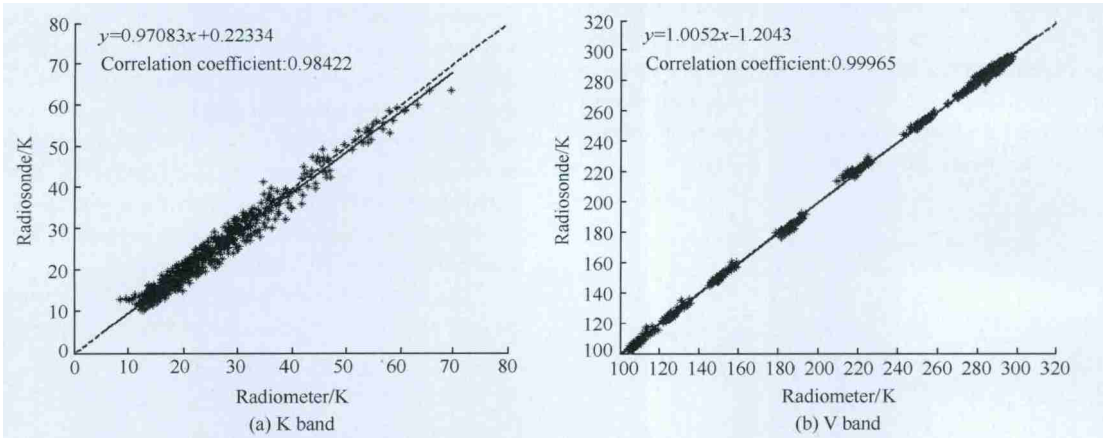

Fig.3 Comparison of radiometer observation brightness temperature and sounding analog brightness temperature

4.2 Analysis of neural network retrieval accuracy

Aside from the optimization of the network design, 12 years (from 2000 to 2011) of historical weather data from Beijing south sounding stations were used as input and the atmosphere temperature and water vapor profile were used as output to allow the BP neural network to achieve acceptable universality and robustness. The large amount of historical sounding data used as the training sample provided the neural network algorithm with a priori information as much as possible. However, a certain difference existed between the simulated brightness temperature from the sounding data calculation and the brightness temperature measured by the radiometer. This difference could affect the inversion result. Therefore, a comparison between the sounding observations and the temperature and water vapor inverted by trained neural network was conducted and the results are shown in Fig. 4.

Fig. 4 shows that the average error of the temperature profile was almost less than 2 K. Mean square error was relatively large when close to the ground, which was below 1 km, and became larger when the height increased. Similarly, the error in the water vapor was relatively large when close to the ground but became small when the height increased. The overall deviation was basically within 1.5 g/m^3, which could be the result of the test sites being approximately 17 km away from the sounding station. A number of differences in the atmospheric environment between the two sites in near-surface may be the main causes of error. At the same time, water vapor was not directly included in the measured sounding values, and instead, was calculated using temperature and other data from the experience model (Chen, 1989; Cao, et al., 2011; Iassamen, et al., 2009), these also resulted in a certain error, which increased the difference between observation and sounding water vapor. In addition, it took about half an hour for the weather balloon to rise to a height of 10 km and to flap randomly with the airflow. Thus, ensuring that

the weather balloon only detects sounding station i nformation at the top of the atmosphere is difficult.

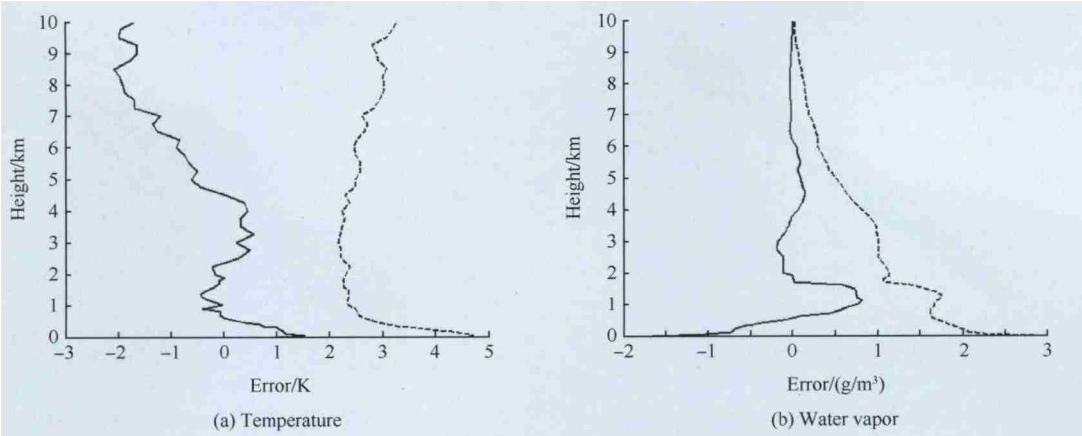

Fig.4 Neural network inversion of atmospheric temperature and water vapor profile error

The temporal resolution of the radiometer observations was higher with an observation for just one minute at the same field. Furthermore, differences existed between the weather background and historical samples during the observation period. These differences were resulted in the differences between radiometer inversion profile and the profile detected by the sounding balloon.

Apart from the sounding results, we likewise compared the observations of our radiometer with those of the MP-3000A foundation multichannel microwave radiometer produced by USA. The difference between sounding observations was analyzed. The MP-3000A and our instruments were installed in the same position for the comparison.

Fig. 5(a) (b) show the mean variations between observed temperature from MP-3000A and the sounding results were larger than 2 K within 1—6 km. Almost all the mean square deviations were greater than 3 K, which was slightly larger than the inversion mean square deviation using our method. Moreover, the observed error of the water vapor is also close to our inversion results. The Result also further shows that our inversion of atmospheric temperature and water vapor were closer to the r adiosonde observations, the inversion results were accurate and reliable. This result may be because the sample selection and the design of the neural network structure are relatively different from the U. S. MP-3000A microwave radiometer, which is more suitable for Beijing's specific circumstances. The mean square e rror of temperature and water vapor was relatively larger in near-surface, which was also observed by MP-3000A.

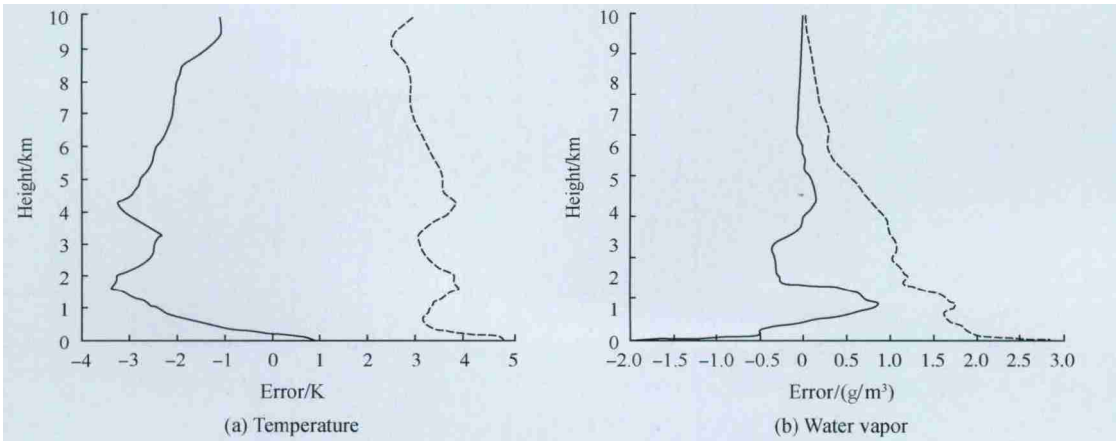

Fig.5 MP-3000 observations of atmospheric temperature and water vapor profiles error

To verify the correlation between inversion parameters and radiosonde observations, we further conducted a linear regression analysis using the temperature and water vapor between inverted profiles and radiosonde profiles. A good agreement was achieved, and the correlation coefficients of temperature and water vapor were 0. 99286 (Fig. 6) and 0. 9153 (Fig. 7) , respectively. The temperature and water vapor fitting line slopes were 0. 9912 and 0. 9801, respectively, with the slope closer to 1. The inversion results and radiosonde observations were almost the same. H owever, the result is less satisfactory in terms of the temperature vapor phase-correlation, which further illustrates the complexity of water vapor stratification in the atmosphere leading to a certain degree of retrieval error.

The accuracy of inverted temperature and water vapor pro-

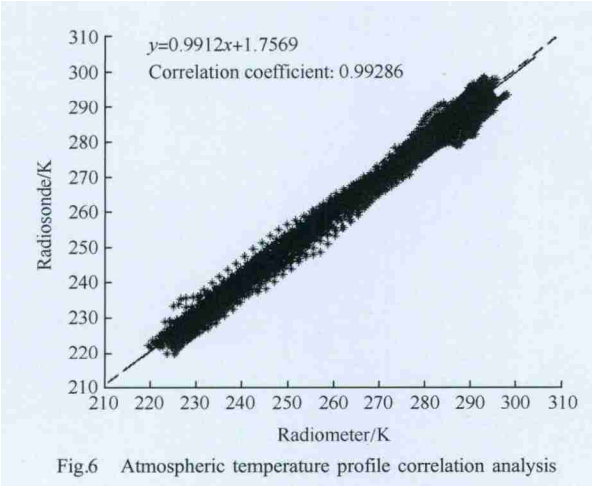

Fig.6 Atmospheric temperature profile correlation analysis

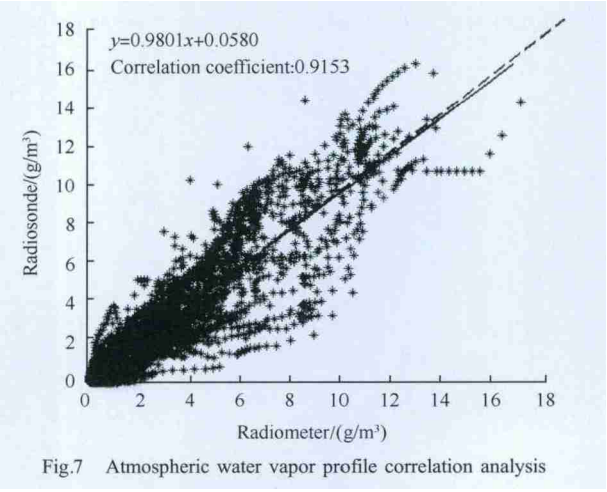

Fig.7 Atmospheric water vapor profile correlation analysis

files with microwave radiometer observations using neural network inversion is limited by historical radiosonde data, microwave radiometer brightness temperature measurement accuracy, radiative transfer model selection, parameter settings, neural network model of the design, and many other factors (Liu, et al., 2010; Westwater, et al., 2003). The training samples used in our test were history radiosonde data obtained in 12 years. However, these data did not cover all weather phenomena, particularly a number of extreme weather conditions that led to some errors in the inversion results. Thereby, improving the accuracy of the retrieval of atmospheric profile parameters is necessary to enhance the universality of neural networks.

Fig. 8(a) (b) show the atmospheric temperature and humidity profiles extracted from the neural network inversion and radiosonde data. Based on the comparison results, the temperature profile was closer to the actual radiosonde data with smaller error. Although some errors were observed in the water vapor and relative humidity profiles, the inversion profiles accurately described the Relative Humidity (RH) and height trends of a tmospheric water vapor and numerical changes. These results also prove the validity and accuracy of the neural network inversion results.

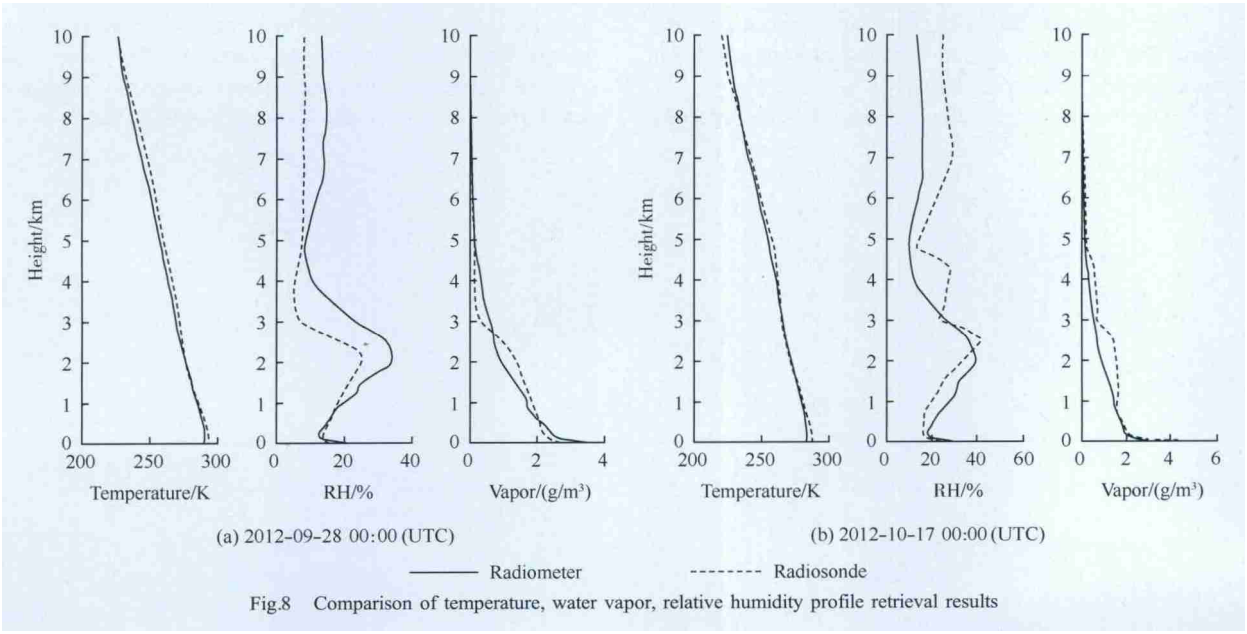

Fig.8 Comparison of temperature, water vapor, relative humidity profile retrieval results

5 CONCLUSION

Through the above experimental results analysis, a novel, self-developed multi-channel foundation microwave radiometer that accurately measures atmospheric radiation brightness temperature is proposed. This proposed radiometer can accurately obtain real-time air temperature, water vapor, relative humidity, and other atmospheric profile information with neural network algorithm as well. The new, ground-based multi-channel microwave radiometer observations are accurate and reliable. In this light, the proposed radiometer can fill the technology gaps in the development of ground-based microwave radiometers in China, provide additional knowledge in related technologies, and reduce the technology gap with similar products from foreign countries. Moreover, the proposed radiometer provides an effective and valuable decision support in terms of numerical weather prediction,

weather modification, disaster prevention and mitigation, and other related fields.

REFERENCES

Cao Y J, Liu J M, Liang H and Chu Y L. 2011. Water vapor resource vertical stratification characteristics retrieved basing on the radiosonde datum. Journal of Natural Resources, 26(9): 1603 – 1612

Cerewell S, Czekala1 H, Lohnert U and Simmer C. 2001. Microwave r adiometer for cloud carthography: a 22-channel ground-based microwave radiometer for atmospheric research. Radio Science, 36(4): 621 – 638 [DOI: 10.1029/2000RS002396]

Chen H Y. 1989. The application of radiosonde data to data processing of microwave radiometer. Journal of Academy of Meteorological Science, 4(2): 186 – 192

Clough S A, Shephard M W, Mlawer E J, Delamere J S, Iacono M J, Cady-Pereira K, Boukabara S and Brown P D. 2004. Atmospheric radiative transfer modeling: a summary of the AER codes. Journal of Quantitative Spectroscopy and Radiative Transfer, 91(2): 233 – 244 [DOI: 10.1016/j. jqsrt. 2004. 05. 058]

Domenico C, Westwater E R, Gasiewski A J and Klein M. 2007. The ground-based scanning radiometer: a powerful tool for study of the arctic atmosphere. IEEE Transactions on Geoscience and Remote Sensing, 45(9): 2759 – 2777 [DOI: 10. 1109/TGRS. 2007. 897423]

Iassamen A, Sauvageot H, Jeannin N and Ameur S. 2009. Distribution of tropospheric water vapor in clear and cloudy conditions from microwave radiometric profiling. Journal of Applied Meteorology and Climatology, 48(3): 600 – 615 [DOI: 10.1175/2008JAMC1916. 1]

Liu H Y, Li J, Cao X Y and Xiong B. 2007. Characteristics of the atmosphere remote sensed by ground-based 12-channel radiometer. Remote Sensing Technology and Application, 22(2): 222 – 229

Liu Y Y, Mao J T, Li J and Li F. 2010. Research of BP neural network for microwave radiometer remote sensing retrieval of Temperature, Relative Humidity, Cloud Liquid Water Profiles. Plateau Meteorology, 29(6): 1514 – 1523

Van Meijgaard E, Baltink H K, Groβ S and Boers R. 2007. Accuracy assessment of an integrated profiling technique for operationally deriving profiles of temperature, humidity, and cloud liquid water. Journal of Geophysical Research, 112 (D4) [DOI: 10. 1029/2006JD007379]

Marzano F S, Cimini D and Ware R. 2005. Monitoring of rainfall by ground-based passive microwave systems: models, measurements and applications. Advances in Geosciences, 2: 259 – 265 [DOI: 10. 5194/adgeo – 2 – 259 – 2005]

Shi Y, Han L Q, Lian X Q. 2009. Neural network design methods and case analysis. Beijing: Beijing University of Posts and Telecommunications Press

Westwater E R, Stankov B B, Cimini D, Han Y, Shaw J A, Lesht B M and Long C N. 2003. Radiosonde humidity soundings and microwave radiometers during nauru99. Journal of Atmospheric and Oceanic Technology, 20(7): 953 – 971 [DOI: 10. 1175/1520 – 0426(2003) 20 < 953: RHSAMR > 2. 0. CO; 2]

Yao Z G and Chen H B. 2005. Analysis of the remote sensing of atmospheric temperature profiles using the seven channel microwave radiometer. Journal of the Meteorological Sciences, 25(2): 133 – 141

Zhang X. 2011. Microwave Radiomeer Remote Sensing Atmospheric Temperture and Humidity Profile in Yangjiang. Nanjing University of Information Science and Technology

Zhao L, Ma Y F, Zhang G X and Yang L M. 2009. The principle and error analysis of microwave radiometer MP-3000A. Desert and Oasis Meteorology, 3(5): 54 – 57

多通道地基微波辐射计大气遥感

雷连发，卢建平，朱磊，吴皓

西安电子工程研究所，陕西 西安 710100

摘 要: 本文主要介绍了自主研发的多通道地基微波辐射计观测亮温和数据反演方法,并与探空观测值进行对比,分析了辐射计观测亮温、反演的温度和水汽廓线的精度。结果表明,该仪器亮温观测误差小且利用神经网络反演的大气温度及水汽等廓线参数准确可靠,具有实际应用价值。

关键词: 微波辐射计,BP 神经网络,MonoRTM 模型,多通道,地基

中图分类号: P407.7 文献标志码: A

引用格式: 雷连发,卢建平,朱磊,吴皓. 2014. 多通道地基微波辐射计大气遥感. 遥感学报,18(1): 180 - 191

Lei L F, Lu J P, Zhu L and Wu H. 2014. Atmospheric remote sensing using multi-channel ground-based microwave radiometer. Journal of R emote Sensing, 1 8(1): 180 - 191 [DOI: 10.11834/jrs.20133013]

1 引 言

大气温度、水汽、相对湿度和云液态水廓线是描述大气状态的基本参数,实时探测这些大气状态参数的时空分布变化,对于数值天气预报和气候变化研究及各种气象保障工作,都必不可少(刘亚亚等,2010)。传统的探测手段主要以探空气球为主,而探空气球又受到使用时间和空间范围的诸多因素限制。地基微波辐射计是观测对流层大气温度、水汽和云等大气参数的新型设备,不仅能够弥补传统常规大气探测资料的不足,克服常规大气探测在应用中存在的某些局限性,而且还能够获得在研究大气结构等方面有价值的气象资料,是大气探测的重要手段之一(张曦,2011; Meijgaard 等,2007)。微波辐射计主要应用于中小尺度天气现象的观测,可连续自动地获取对流层的大气温度、相对湿度、水汽以及液态水等大气参数,这对于天气预报、人工影响天气、防洪指挥决策、大气环境研究等有重要意义(赵玲 等,2009)。它还具有独立工作的能力,可全天时、全天候地工作并且具有穿透云雾的能力,非常适合于自动气象站配置。为了提高短期预报和空气污染的监测能力,得到连续的大气垂直结构是非常重要的。地基微波辐射计可以获取连续的温度、相对湿度、水汽以及液态水等廓线信息的观测是非常有价值的(刘红燕 等,2007)。

地基微波辐射计数据反演主要是利用观测的亮温来反演大气温度、水汽、相对湿度和云液态水等大气参数。反演方法有正向模型反演法、数据统计法(经验法)和人工神经网络法等。深入分析表明从微波辐射计数据获取温度、水汽和云液态水廓线的方法中,人工神经网络方法更胜一筹,它具有很多传统算法不具有的特点。理论上已经证明 3 层神经网络具有以任意精度逼近任何复杂非线性模型的能力,神经网络不必要分析复杂的物理模型(刘亚亚 等,2010; 施彦 等,2009),可直接利用历史数据对网络进行训练。该方法具有较好的自学习能力及处理非线性问题的能力,在大气科学研究等领域越来越受到重视。

2 微波辐射计简介

微波辐射计是一款被动式的微波遥感设备,它本身并不发射电磁波,而是通过被动地接收被观测场景辐射的微波能量来探测目标的特性。

大气对微波具有选择性吸收的特性。图 1 表示了大气中云、水汽和氧气的吸收光谱。从图 1 中

收稿日期: 2013-01-23; 修订日期: 2013-07-09; 优先数字出版日期: 2013-07-16

基金项目: 公益性行业(气象)科研专项(编号: GYHY201006030)

第一作者简介: 雷连发(1985—),男,硕士研究生,现从事大气遥感应用研究。E-mail: leilianfa_2006@163.com

可以看出,22 GHz 处的特征表现为一个水汽谐振带,60 GHz 处的特征表现为大气氧气的谐振带集合,所以通过测量水汽和氧气在 22 GHz 和 60 GHz 附近的大气辐射强度或亮温就可以反演出大气水汽和温度的垂直分布(Marzano 等,2005; 姚志刚 等,2005)。在微波辐射计数据反演中通过采用人工神经网络方法并结合大量历史探空资料就可以反演高精度的大气廓线参数(Cerewell 等,2001; Domenico 等,2007)。

本文采用自主研发的新型多通道地基微波辐射计进行大气特性参数遥感探测。该微波辐射计是用于地表上空大气环境连续监测的精密探测仪器,对大气对流层辐射特性的深入研究。系统设置了 35 个大气探测频率点,其中在 K 频段(22—30 GHz)有 21 个探测频点,在 V 频段(51—59 GHz)有 14 个探测频点。仪器通过对这 35 个频率点进行扫描接收,以完全被动的探测方式准确测量并获取大气辐射亮温值。最后利用人工神经网络算法并结合大量无线电历史探空资料,不仅可以探测得到大气柱水汽和液态水含量,还能实时反演获得连续、高分辨率的大气温度和水汽廓线等大气参数。这为数值天气预报和人工影响天气作业等提供了重要的观测数据和决策支持。

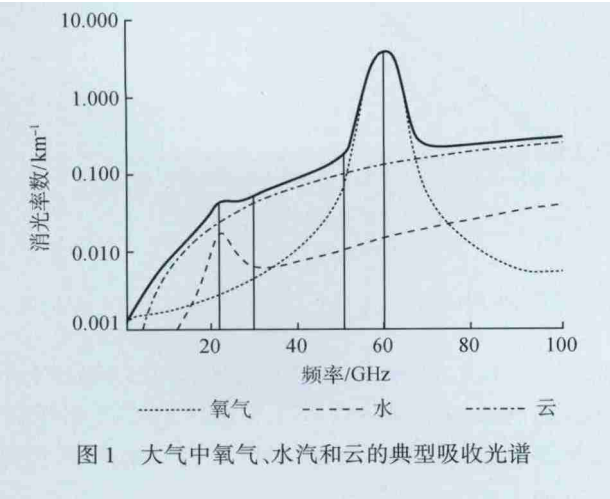

图 1 大气中氧气、水汽和云的典型吸收光谱

3 神经网络设计与分析

本文使用的 Back Propagation (BP) 神经网络反演方法采用 3 层误差反向传播 BP 神经网络模型算法,该算法使用广泛且较为成熟。在神经网络训练过程中本文将地面观测的气象参数(包括地面温度、气压、相对湿度)以及辐射计观测的各频点亮温作为输入,对应于不同的网络。温度、相对湿度、云液态水廓线的各 58 个节点分别作为输出。网络参数训练时选用当地大量探空资料作为训练样本进行网络训练,最终得到一组最佳匹配的网络参数。训练后的网络就可直接用于微波辐射计的大气温度、水汽、液态水等廓线反演。本次实验观测地点是位于北京市的中国国家气象局内,从 2012 年 9 月上旬至 2012 年 11 月上旬进行了为期两个月的连续观测实验。通过利用北京南郊探空气象站的历史探空数据进行神经网络训练并进行了仪器观测数据反演和精度分析。

4 实验结果分析

4.1 观测亮温分析与比较

探空数据没有直接测量的亮温数据,需要通过大气辐射模型进行亮温模拟计算。本文选用 MonoRTM 大气辐射模型进行亮温的模拟计算(刘亚亚 等,2010; Clough 等,2004)。由于探空观测仅每天早晚各一次,数据量有限,而且探空气球上升到 10 km 高度大约需要 30 min,因此选取探空时段辐射计输出亮温的平均值与探空数据模拟计算的亮温进行对比分析。观测值与真值(探空模拟计算)平均偏差(*BIAS*)和均方差(*RMS*)被定义为

$$BIAS = \frac{1}{n}\sum_{i=1}^{n}\left(X_{i,\mathrm{meas}} - X_{i,\mathrm{true}}\right) \quad (1)$$

$$RMS = \sqrt{\frac{1}{n}\sum_{i=1}^{n}\left(X_{i,\mathrm{meas}} - X_{i,\mathrm{true}}\right)^2} \quad (2)$$

式中,n 表示观测样本数,$X_{i,\mathrm{meas}}$ 和 $X_{i,\mathrm{true}}$ 分别表示观测值和真值。本次实验在 2012 年 9 月 10 日至 10 月 20 日之间共选取晴空条件下辐射计与探空同时刻 69 组探测数据样本进行了对比分析。图 2(a)(b)分别表示了观测亮温与模拟亮温在 K 频段和 V 频段的平均偏差和均方差。

从图 2 对比结果可以看出 K 频段平均偏差基本都小于 1 K,仅有在水汽吸收峰处偏差在 1.6 K,这主要是由于在水汽吸收峰处受到水汽的影响较大,同时在利用 MonoRTM 模型计算亮温时需要利用经验模式估算可降水量和云中液态水含量(陈宏尧,1989),由于这些估算方法的局限性使得估算结果不够准确,这样就会对亮温的模拟计算精度带来一定的影响,使得这些频点平均偏差较大。对于 V 频段来说尽管测量误差相对于 K 频段偏大,但平均相对偏差都小于 2.5%,相对较小。

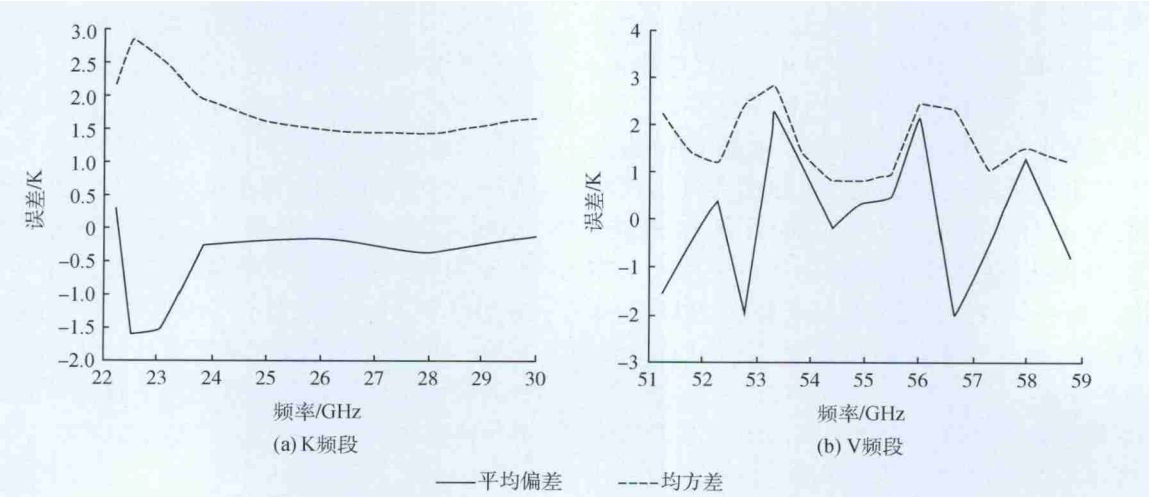

图 2 辐射计观测亮温与探空模拟亮温的平均偏差和均方差

图 3(a)(b)分别表示了辐射计在 K 频段和 V 频段观测的大气辐射亮温与计算的探空模拟亮温之间的线性相关性。从结果可以看出两者线性关系较好,具有较高的一致性。通过比较可以看出该微波辐射计亮温观测值的准确性是可信的,它的准确性会直接影响到后续神经网络反演算法的精度,因此仪器应尽可能地提高抗噪能力和观测精度。

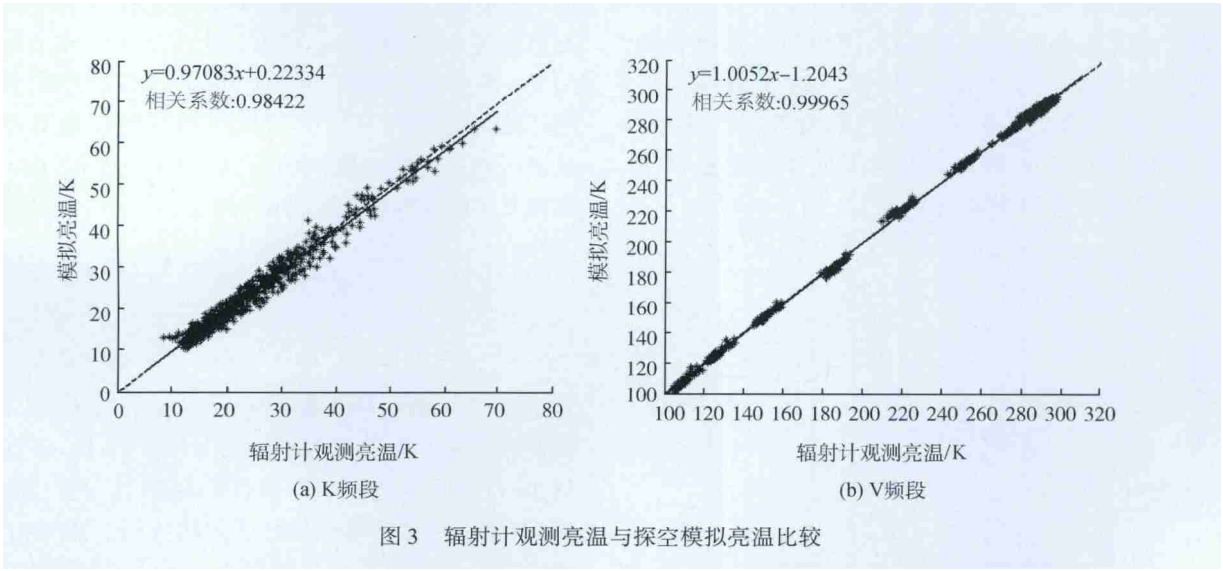

图 3 辐射计观测亮温与探空模拟亮温比较

4.2 神经网络反演廓线精度分析

为了使 BP 神经网络具有较好的普适性和鲁棒性,除了对网络设计本身的优化外还在网络训练时选用北京南郊探空气象站 2000 年—2011 年共 12 年的大量历史探空资料来计算模拟亮温值作为网络输入参数,将探空的大气温度和湿度廓线等作为网络输出值进行训练。选用大量历史探空数据作为训练样本为神经网络算法提供尽可能多的先验信息。然而利用探空数据计算的模拟亮温值和辐射计实测亮温值存在一定的差异,这就会对反演结果带来一定的影响,为此本文用训练好的神经网络对仪器观测的亮温进行了大气温度和水汽廓线的反演并和探空结果作对比,计算了温度廓线和水汽廓线的平均误差和均方差如图 4 所示。

从图 4 中可以看出温度廓线平均误差基本都小于 2 K,均方差在近地面 1 km 以下相对较大,在高空随高度上升略有变大。同样水汽也是近地面误差相对较大,而高空误差较小,整体偏差基本都在 1.5 g/m^3 以内。近地面误差大是由于实验地点选在国家气象局内,距离探空站的直线距离有 17 km 左右,两地近地面大气环境存在一定的差异,这

可能是引起近地面误差较大的主要原因之一。同时探空资料中并没有直接的水汽测量值,而是利用温度等通过经验模式计算得到的(陈宏尧,1989; 曹玉静 等,2011; Iassamen 等,2009),这也会带来一定的误差,使得仪器观测结果与探空水汽的差异变大。此外探空气球上升到 10 km 的高度大约需要半个小时,并随着气流随意飘动,难以保证它只探测探空站上方的大气信息,而辐射计观测的时间分辨率较高,每分钟一条数据且始终探测同一视场,而且观测期间的天气背景与历史样本也可能存在差异,这都是造成辐射计反演廓线与探空气球探测的大气参数廓线存在一定差异的原因。

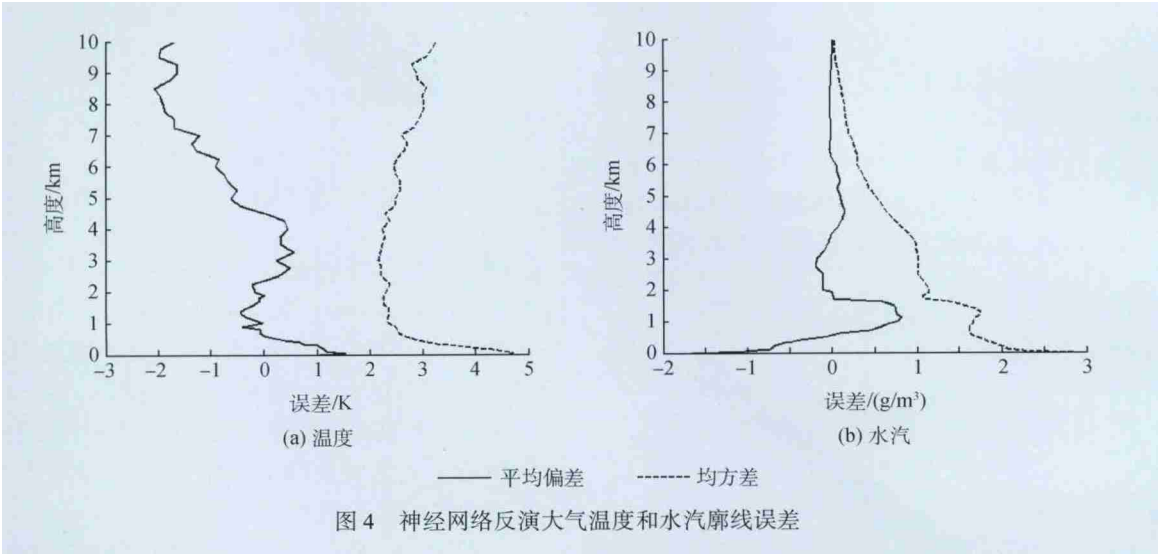

图 4 神经网络反演大气温度和水汽廓线误差

在与探空结果比较的同时本文还将该辐射计的观测结果与美国生产的 MP-3000A 地基多通道微波辐射计的观测结果做了比较,分析了其与探空观测结果的误差。这台 MP-3000A 微波辐射计与本文中的仪器安装在同一位置,因此具有一定的可比性。

从图 5(a)和(b)可以看出美国 MP-3000A 微波辐射计观测的温度与探空结果的平均偏差在 1—6 km 范围内大于 2 K,而均方差基本都大于 3 K,略大于本文的反演误差,水汽的观测误差与本文的反演结果较为相近。这也进一步说明我们反演的大气温度和水汽较接近于探空观测值,反演结果是准确可靠的。这可能是由于本文在样本的筛选以及神经网络结构的设计等方面与美国 MP-3000A 微波辐射计存在较大差异,可能更适合北京的具体情况。同样 MP-3000A 观测的温度和水汽在近地面均方差也相对较大,这与本文的观测结果相同。

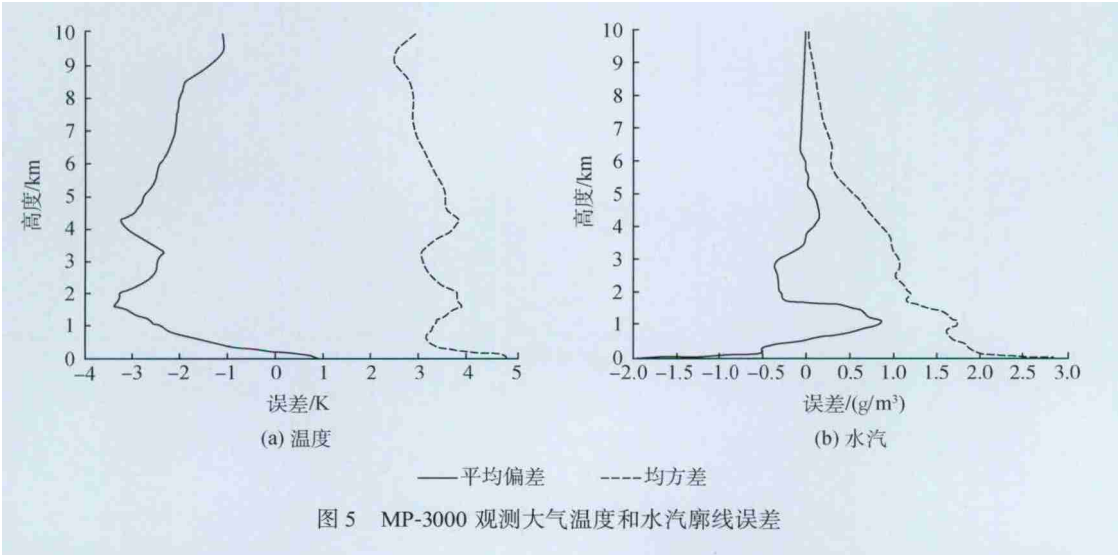

图 5 MP-3000 观测大气温度和水汽廓线误差

为了验证反演参数与探空观测结果的相关性，进一步对69组反演的温度和水汽廓线与探空廓线作线性回归分析，得到两者的相关系数，温度和水汽的相关系数分别为0.99286(图6)和0.9153(图7)。从结果可以看出69组样本反演结果与探空廓线相关性较好，温度和水汽拟合直线斜率分别为0.9912和0.9801，斜率较接近于1，反演结果与探空观测值较接近。水汽相关性相对于温度来说差一些，这也进一步说明了大气中水汽层结的复杂性会导致一定的反演误差。

微波辐射计利用神经网络反演的温度和水汽廓线的精度受到历史探空资料、微波辐射计本身亮温测量的精度、辐射传输模式选择与参数设置、神经网络模型本身的设计等诸多因素的影响(刘亚亚等,2010; Westwater 等,2003)。本文使用的训练样本为近12年的历史探空资料，它并不能涵盖所有天气现象，特别是一些极端的天气情况，这在很大程度上会给反演结果带来一定的误差，因此提高神经网络的普适性和极端天气情况的处理能力有利于提高大气廓线参数的反演精度。

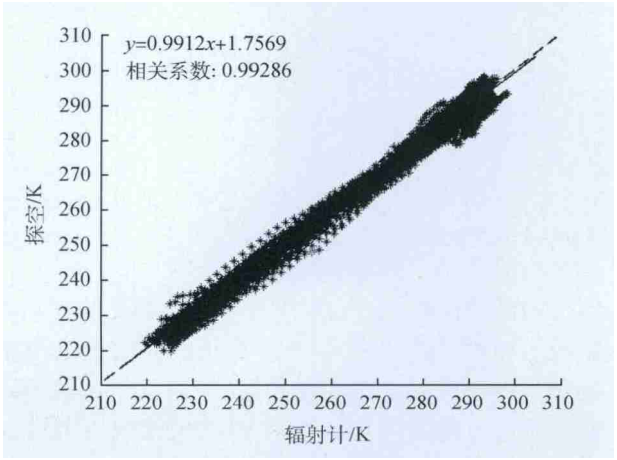

图6 大气温度廓线相关性分析

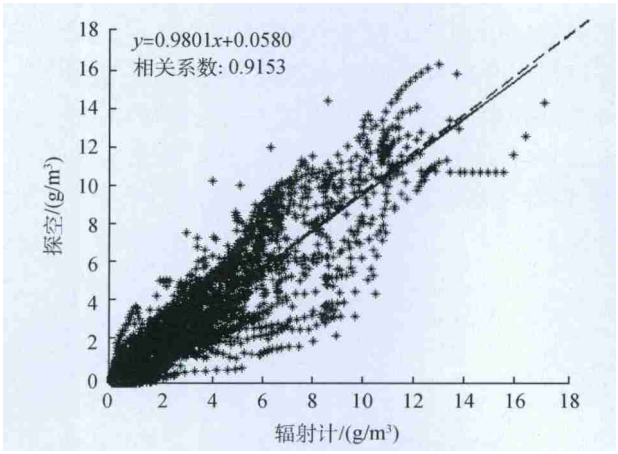

图7 大气水汽廓线相关性分析

图8(a)(b)是利用训练好的神经网络反演的大气温湿廓线与探空数据的对比结果。从对比结果中可以看出温度廓线较接近实际探空数据，误差较小。水汽和相对湿度廓线尽管有一定的误差，但反演廓线很好地描述了大气中水汽和相对湿度随高度的变化趋势以及数值变化情况，这也说明了神经网络反演结果的有效性和准确性。

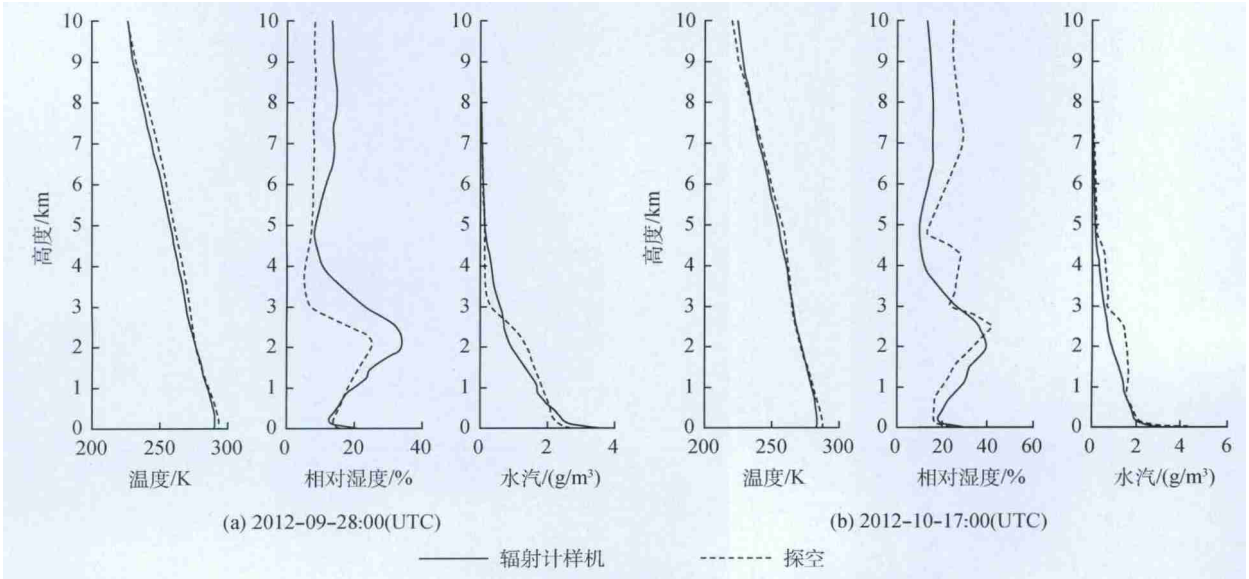

图8 温度水汽相对湿度廓线反演结果对比

5 结 论

通过以上实验结果分析可以看出本文自主研发的新型多通道地基微波辐射计能够准确地测量大气辐射亮温,并结合神经网络算法可以实时准确地获取大气温度、水汽和相对湿度等大气廓线信息。该新型多通道地基微波辐射计观测结果准确可靠,填补了中国在地基微波辐射计技术方面的空白,积累了相关技术经验,缩短了与国外同类产品之间的技术差距,可以为数值天气预报、人工影响天气、防灾减灾等领域提供很好的决策支持,具有很高的实用价值。

参考文献(References)

曹玉静, 刘晶淼, 梁宏, 楚艳丽. 2011. 基于无线电探空资料反演大气水汽资源的垂直层结特征. 自然资源学报, 26(9): 1603-1612

Cerewell S, Czekala1 H, Lohnert U and Simmer C. 2001. Microwave radiometer for cloud carthography: a 22-channel ground-based microwave radiometer for atmospheric research. Radio Science, 36(4): 621-638 [DOI: 10.1029/2000RS002396]

陈宏尧. 1989. 探空资料在微波辐射计资料处理中的应用. 气象科学研究院院刊, 4(2): 186-192

Clough S A, Shephard M W, Mlawer E J, Delamere J S, Iacono M J, Cady-Pereira K, Boukabara S and Brown P D. 2004. Atmospheric radiative transfer modeling: a summary of the AER codes. Journal of Quantitative Spectroscopy and Radiative Transfer, 91(2): 233-244 [DOI: 10.1016/j.jqsrt.2004.05.058]

Domenico C, Westwater E R, Gasiewski A J and Klein M. 2007. The ground-based scanning radiometer: a powerful tool for study of the arctic atmosphere. IEEE Transactions on Geoscience and Remote Sensing, 45(9): 2759-2777 [DOI: 10.1109/TGRS.2007.897423]

Iassamen A, Sauvageot H, Jeannin N and Ameur S. 2009. Distribution of tropospheric water vapor in clear and cloudy conditions from microwave radiometric profiling. Journal of Applied Meteorology and Climatology, 48(3): 600-615 [DOI: 10.1175/2008JAMC1916.1]

刘红燕, 李炬, 曹晓彦, 熊斌. 2007. 遥感大气结构的地基 12 通道微波辐射计测量结果分析. 遥感技术与应用, 22(2): 222-229

刘亚亚, 毛节泰, 刘均, 李峰. 2010. 地基微波辐射计遥感大气廓线的 BP 神经网络反演方法研究. 高原气象, 29(6): 1514-1523

Van Meijgaard E, Baltink H K, Groβ S and Boers R. 2007. Accuracy assessment of an integrated profiling technique for operationally deriving profiles of temperature, humidity, and cloud liquid water. Journal of Geophysical Research, 112 (D4) [DOI: 10.1029/2006JD007379]

Marzano F S, Cimini D and Ware R. 2005. Monitoring of rainfall by ground-based passive microwave systems: models, measurements and applications. Advances in Geosciences, 2: 259-265 [DOI: 10.5194/adgeo-2-259-2005]

施彦, 韩力群, 廉小亲. 2009. 神经网络设计方法与实例分析. 北京: 北京邮电大学出版社

Westwater E R, Stankov B B, Cimini D, Han Y, Shaw J A, Lesht B M and Long C N. 2003. Radiosonde humidity soundings and microwave radiometers during nauru99. Journal of Atmospheric and Oceanic Technology, 20(7): 953-971 [DOI: 10.1175/1520-0426(2003)20<953:RHSAMR>2.0.CO;2]

姚志刚, 陈洪滨. 2005. 七通道微波辐射计遥感大气温度廓线的性能分析. 气象学报, 25(2): 133-141

张曦. 2011. 地基微波辐射计遥感阳江大气温湿廓线的研究. 南京: 南京信息工程大学

赵玲, 马玉芬, 张广兴, 杨莲梅. 2009. MP-3000A 微波辐射计的探测原理及误差分析. 沙漠与绿洲气象, 3(5): 54-57